Catalysis Today 144 (2009) 312–317

Contents lists available at ScienceDirect

Catalysis Today

journal homepage: www.elsevier.com/locate/cattod

Formation of active phases in MoVTeNb oxide catalysts for ammoxidation of propane

G.Ya. Popova [a,*], T.V. Andrushkevich [a], Yu.A. Chesalov [a], L.M. Plyasova [a], L.S. Dovlitova [a], E.V. Ischenko [a], G.I. Aleshina [a], M.I. Khramov [b]

[a] Boreskov Institute of Catalysis SB RAS, Novosibirsk, Russia
[b] Solutia Inc., P.O. Box 97, Gonzalez, FL 32560-0097, USA

ARTICLE INFO

Article history:
Available online 6 March 2009

Keywords:
MoVTeNb mixed oxide
Catalyst preparation and characterization
Propane ammoxidation

ABSTRACT

The method of drying, heat evaporation or spray drying, of the aqueous suspension of starting chemicals has a pronounced effect on the phase composition of the final MoVTeNb catalyst, which ultimately influences the catalytic properties in propane ammoxidation reaction. The sample synthesized by spray drying is active and selective; it contains two main crystalline phases, orthorhombic M1 and hexagonal M2. The activity of the sample prepared by heat evaporation is low. This sample does not contain the active M1 phase and consists of hexagonal M2, $TeMo_5O_{16}$, and $Mo_{5-x}(V/Nb)_xO_{14}$ phases. The different mechanisms of phase composition formation in the samples synthesized by heat evaporation or spray drying arise from the different chemical nature of corresponding solid precursors.

1. Introduction

Selective heterogeneous catalytic oxidation of alkanes is a promising method for the production of value-added products from inexpensive and abundant raw materials. During the last decade, the MoVTeNb oxide catalysts developed by Mitsubishi Chemical Corporation have received a lot of attention [1–3]. These catalysts have shown high efficiency in selective oxidation and ammoxidation of propane. Their unique catalytic properties are attributed to the presence of orthorhombic M1 phase, which is responsible for activation of propane [4–7]. Formation of the active phases responsible for selective catalytic transformations of propane is determined by the synthesis conditions and post-synthesis thermal treatment of the material.

High sensitivity of M1 phase formation to some parameters of synthesis such as slurry pH, presence of oxoacids in the starting solution, method of slurry drying, redox conditions during heat treatment [8–12] points to the importance of the nature of precursors in the catalyst preparation process.

The pH of the slurry strongly influences both the crystallinity and the nature of the precursors. Oliver et al. [9] have demonstrated that $(NH_4)_6TeMo_6O_{24}{\cdot}nH_2O$, an Anderson-type heteropolyanion, was formed in samples prepared at pH 3.0–4.5. At pH < 3 the heteropolyanion partially decomposed with the formation of mostly amorphous materials. At a very low pH 1–1.5 polyoxovanadates were also present in the precursors.

Beato et al. [12] studied early stages of the catalyst formation by *in situ* Raman spectroscopy. The interaction between molybdenum, vanadium, and tellurium resulted in favored formation of an Anderson-type heteropolyanion $[TeM_6O_{24}]^{n-}$ (M = Mo, V; $n \geq 6$) and protonated decavanadate species $[H_xV_{10}O_{28}]^{(6-x)-}$. Raman analysis showed that the nature of the Anderson-type tellurate was preserved after addition of the aqueous niobium oxalate solution and the subsequent spray drying of the material. According to the authors [12], niobium affected the crystallinity of the polyoxometallates and acted as a link connecting $[TeM_6O_{24}]^{n-}$ ($n \geq 6$) units even in the solution. The conditions of the drying process were critical as well [8].

In this work we have studied the influence of the method of drying, heat evaporation or spray drying, of aqueous suspension of starting materials on the chemical and phase composition of the solid precursors and of final $MoV_{0.3}Te_{0.23}Nb_{0.12}O_x$ catalyst calcined for 2 h in He flow at 600 °C.

2. Experimental

2.1. Catalyst preparation

$MoV_{0.3}Te_{0.23}Nb_{0.12}O_x$ catalysts were prepared using the ammonium heptamolybdate $(NH_4)_6Mo_7O_{24}{\cdot}4H_2O$ and ammonium metavanadate NH_4VO_3 (chemicals from commercial suppliers in Russia)

* Corresponding author at: Boreskov Institute of Catalysis SB RAS, Lavrentieva str. 5, Novosibirsk, Russia. Tel.: +7 383 3306219; fax: +7 383 3306219.
E-mail address: gyap@catalysis.nsk.su (G.Ya. Popova).

0920-5861/$ – see front matter © 2009 Elsevier B.V. All rights reserved.
doi:10.1016/j.cattod.2009.01.049

and telluric acid H_6TeO_6 (Aldrich); the purity of each reagent was 99% or higher. Niobium oxalate was prepared by hydrolysis of niobium pentachloride ($NbCl_5$, Acros Organics, 99.8%) in water and neutralization with ammonium hydroxide (NH_4OH). The white precipitate was filtered, washed with water and dissolved in a solution of oxalic acid ($C_2O_4^{2-}$/Nb = 3.0).

The flow chart of the catalyst preparation is shown in Fig. 1. An aqueous niobium oxalate solution was added to an aqueous solution of $(NH_4)_6Mo_7O_{24}{\cdot}4H_2O$, NH_4VO_3, and H_6TeO_6 at 30 °C, which resulted in the formation of an orange gel-like slurry.

The following methods of catalysts preparation from the slurry have been examined.

(a) Thermal evaporation method, in which the slurry was dried on an open glass surface on a hot plate at 80 °C; the wet paste was dried on air during 12 h at 110 °C.
(b) Spray-drying procedure, in which a lab spray-dryer (Buchi-290) was used to prepare a solid precursor powder; the inlet temperature was 190 °C and the outlet temperature was 130 °C.

The resulting solid precursors were calcined in a He flow at 600 °C for 2 h. In the text below the catalysts are referred to as D_x (heat evaporation method) or R_x (spray drying), where **x** is the temperature of the heat treatment.

2.2. Catalyst characterization

The specific surface areas of catalysts were determined by low temperature nitrogen adsorption at 77 K using an automatic ASAP-2400 apparatus.

Powder XRD diffraction patterns were recorded using a Siemens D500 diffractometer and Cu K_α radiation with 0.02° (2Θ) steps over the angular range 5–70° with 16 s counting time per step.

IR spectra were recorded using an FT-IR spectrometer BOMEM MB-102. The samples were pretreated by a standard method of pelletizing with CsI (2 mg of the sample and 500 mg of CsI), before the spectra were recorded.

Raman spectra were recorded using an FT-Raman spectrometer RFS 100/S BRUKER. The excitation source was 1064 nm line of Nd-YAG laser operating at power level of 100 mW.

The chemical composition of compounds formed in the catalysts was determined by a differential dissolution method (DD) [13,14]. The DD method consists in dissolving the sample under analysis in an appropriate solvent, the concentration (or chemical potential) of which increases during the dissolution. The procedure makes it possible to dissolve progressively and selectively the compounds that make up the analyzed sample, and express the kinetics of dissolution as the curves of release of the analyzed chemical elements into the solvent. To find the chemical formulas of the dissolving compounds, and their quantities, the original kinetic curves of dissolving elements are transformed into stoichiograms, which represent the molar ratios of the element dissolution rates versus time. Such stoichiograms make it possible to derive chemical formulas of the analyzed compounds, and the curves of the compounds dissolution allow determination of the quantities of these compounds. The concentration of dissolved V, Mo, Nb, and Te in the solvent flow was determined by means of an ICP atomic emission analyzer (ICP, Baird). Water, HCl (1.2 and 3N), and HF (3.8N) were consecutively used as the solvents. The temperature of the solvent was gradually increased from 60 to 80 °C.

2.3. Catalytic tests

The catalyst test experiments were carried out at atmospheric pressure in a fixed-bed tubular reactor (i.d. 12 mm; length 50 mm) with a coaxial thermocouple pocket (i.d. 4 mm). Catalyst samples (0.25–0.50 mm particle size) were charged into the reactor and diluted with an inert material. The reactor was mounted in an air-heated furnace. The temperature change along the furnace height was ±2 °C. The reaction temperature was measured using a thermocouple placed in the thermocouple pocket directly in the catalyst bed. A mixture of propane, ammonia and air was passed through the reactor with the catalyst. Propane was 99.9% pure. Before operation, the reactor with the catalyst was heated in a helium flow to the required temperature.

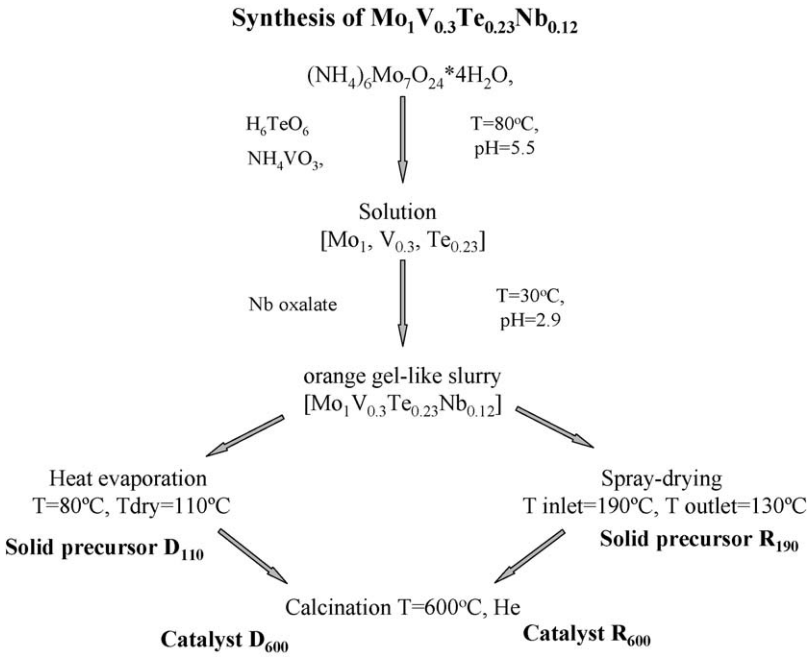

Fig. 1. Flow chart of the catalyst preparation process.

Table 1
Catalyst characterization.

Sample	Chemical composition	S ($m^2\ g^{-1}$)
D_{110}	$Mo_1V_{0.3}Te_{0.23}Nb_{0.12}$	–
D_{600}	$Mo_1V_{0.3}Te_{0.16}Nb_{0.12}$	5.4
R_{190}	$Mo_1V_{0.3}Te_{0.23}Nb_{0.12}$	–
R_{600}	$Mo_1V_{0.3}Te_{0.12}Nb_{0.12}$	7.3

The catalyst performance was compared at a constant composition of the reaction mixture with a molar ratio C_3H_8/NH_3/air = 1/1.2/15 at 420 °C. Reactants and products were analyzed using online gas chromatography.

3. Results

3.1. Catalyst characterization

Table 1 illustrates the effect of the slurry drying method on the physicochemical characteristics of the final catalysts (D_{600} and R_{600}).

Specific surface area of D_{600} sample was 5.4 $m^2\ g^{-1}$, and that of R_{600} sample was 7.3 $m^2\ g^{-1}$. After heat treatment at 600 °C the mole ratio Te/Mo decreased from 0.23 to 0.16 in D_{600} and to 0.12 in R_{600} sample. The differences in the tellurium content of the final catalysts could be explained by the differences in the phase composition and surface. The catalyst prepared by heat evaporation method included primarily M2 phase characterized by enhanced Te/Mo ratio ($Te_{0.33}MO_{3.33}$, M = Mo, V, Nb). The sample prepared by spray drying consisted primarily of M1 phase ($Te_2M_{20}O_{57}$, M = Mo, V, Nb) [4] (Fig. 4). Due to tellurium volatility at high temperature, the lower tellurium content of the sample prepared by spray drying could be attributed to a larger surface.

3.2. Catalytic performance in the propane ammoxidation

Catalytic properties of the samples after heat treatment at 600 °C are shown in Figs. 2 and 3. The products of propane transformation were acrylonitrile, propylene, acetonitrile, acrylic acid, HCN, CO, and CO_2. Carbon balance was 98 ± 2%.

The method of the slurry drying had a strong effect on the activity and selectivity of MoVTeNb mixed oxide catalysts.

Fig. 2 illustrates the effect of the method of slurry drying on the activity determined as the propane conversion rate constants calculated using the first order equation. The D_{600} sample was considerably less active than R_{600} sample. The propane conversion rate constant for R_{600} was 0.65 ml $g^{-1}\ s^{-1}$ compared to 0.07 ml $g^{-1}\ s^{-1}$ for D_{600} sample.

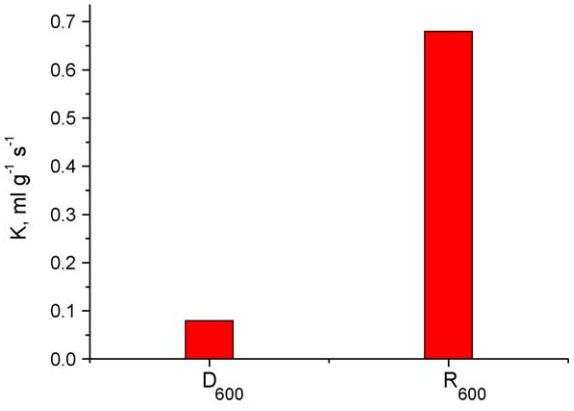

Fig. 2. The propane conversion rate constants observed during propane ammoxidation on D_{600} and R_{600} samples. Reaction temperature 420 °C.

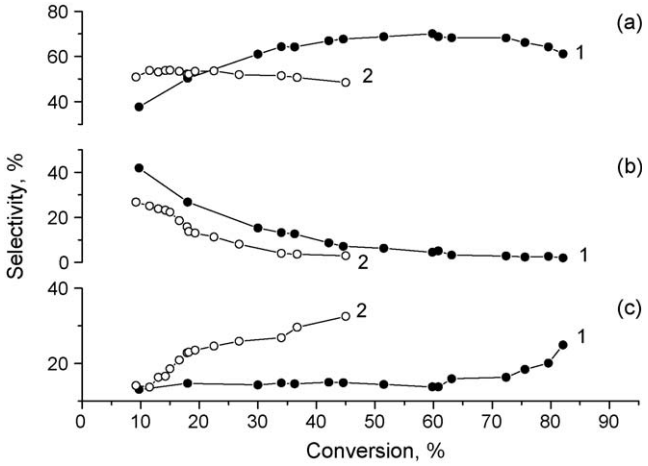

Fig. 3. Selectivities to acrylonitrile (a), propylene (b), and CO_x (c) versus propane conversion for samples R_{600} (1: dark points) and D_{600} (2: light points). Reaction temperature 420 °C.

The propane selectivities to acrylonitrile as a function of propane conversion on R_{600} and D_{600} catalysts are shown on Fig. 3. As propane conversion on R_{600} catalyst increased from 10 to 45%, the selectivity to acrylonitrile increased from 40 to 70%, and selectivity to C_3H_6 decreased from 45 to 10%. Selectivity to CO_x remained nearly constant, 12–14%, in this propane conversion range. Increasing selectivity to acrylonitrile with decreasing selectivity to propylene suggests a consecutive (via propylene) mechanism of acrylonitrile formation [15]. In the propane conversion range from 40 to 75% the selectivities to acrylonitrile and to propylene varied moderately and were equal to ca. 70 and 10%, respectively. Further increase of propane conversion resulted in a decrease of selectivity to acrylonitrile and an increase of selectivity to CO_x.

Low activity of D_{600} catalyst complicates the study of this catalyst at high propane conversion. In the range of propane conversion from 10 to 40% the selectivity to acrylonitrile was practically constant and equal to about 50%, whereas the selectivity to C_3H_6 sharply decreased and selectivity to CO_x significantly increased.

The differences in the catalytic properties of D_{600} and R_{600} samples could be attributed to their different phase compositions. Hexagonal M2, $TeMo_5O_{16}$, and $Mo_{5-x}(V/Nb)_xO_{14}$ phases were present in D_{600} sample (Fig. 4a). In catalytically active and selective sample R_{600}, two main crystalline phases, orthorhombic M1 and hexagonal M2, were present (Fig. 4b).

3.3. Precursor characterization

3.3.1. XRD

The drying method of the slurry had a strong effect on the structural composition of the solid catalyst precursor. The XRD pattern of D_{110} solid precursor (Fig. 5a) had peaks at 2Θ = 10.3, 12.5, 13.1, 16.0, 18.1, 23.2, 25.0 and 27.8, which suggested the presence of Anderson-type heteropolyanion $(NH_4)_6TeMo_6O_{24}{\cdot}7H_2O$ [19] and/or $(NH_4)_7TeMo_5VO_{24}{\cdot}8H_2O$ [20]. The R_{190} solid precursor was amorphous to X-rays (Fig. 5b); only a single broad peak in the angular range of $2\Theta = 27.0^\circ$ was observed in the XRD pattern.

3.3.2. The differential dissolution method (DD)

The chemical compositions of compounds present in the precursors were determined by a differential dissolution method (DD) [13,14].

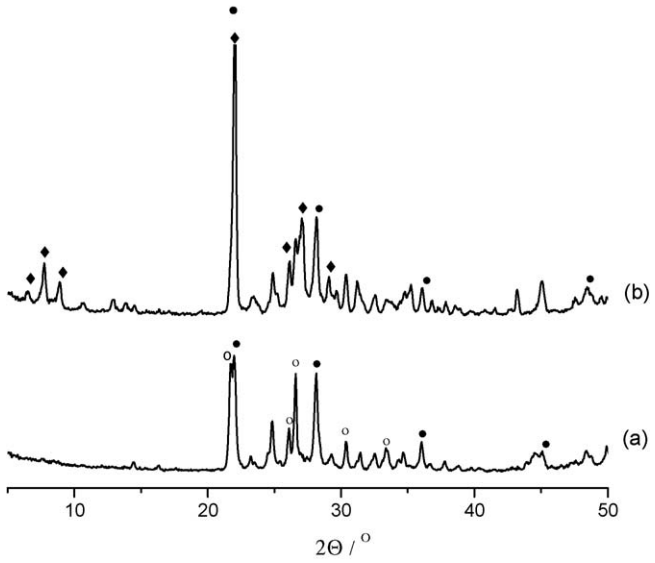

Fig. 4. XRD patterns of samples after heat treatment: (a) D_{600} and (b) R_{600}. (●) M2 (2Θ = 22.0, 28.2, 36.1, 45,0 and 50) [15]; (○) $TeMo_5O_{16}$ (2Θ = 21.9, 26.2, 26.6 and 30.5) [16]; (□) $Mo_{5-x}(V/Nb)_xO_{14}$ (2Θ = 14.4, 16.4, 22.1, 23.3, 24.8, 29.4, 32.6 and 34,7) [17]; (◆) M1 (2Θ = 6.5, 7.7, 9.0 and 27.2) [18].

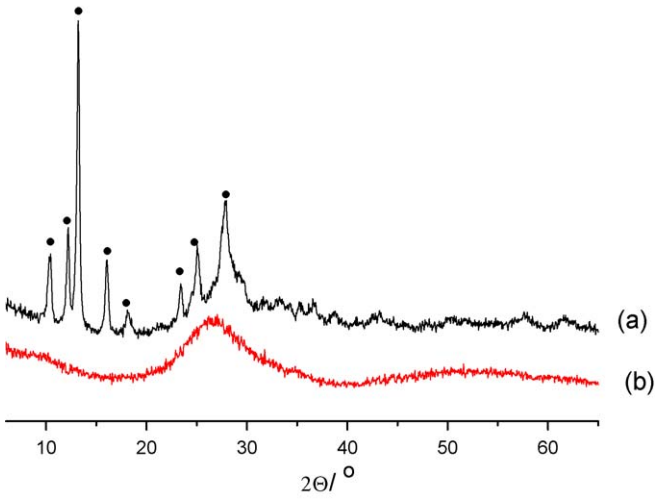

Fig. 5. XRD patterns of the solid precursors: (a) D_{110} and (b) R_{190}. (●) $(NH_4)_6TeMo_6O_{24}\cdot 7H_2O$ and/or $(NH_4)_7TeMo_5VO_{24}\cdot 8H_2O$.

Fig. 6 shows the dissolution curves of Mo, V, Te, Nb and the corresponding stoichiograms (V/Mo, Te/Mo and Nb/Mo) as a function of the dissolved amount of the sample (in relative percentages).

Water, HCl (1.2 and 3N) and HF (3.8N) were consecutively used as solvents. During dissolution of D_{110} solid precursor in water, molybdenum, vanadium, and tellurium went into the solution (Fig. 6, left). The V/Mo and Te/Mo stoichiograms were constant, which indicates the dissolution of a compound with the composition $Mo_1V_{0.28}Te_{0.15}O_n$. During dissolution in water of R_{190} solid precursor, all four components (molybdenum, vanadium, tellurium and niobium) went into the solution (Fig. 6, right). The V/Mo, Te/Mo and Nb/Mo stoichiograms were constant, which indicates the dissolution of a compound with the composition $Mo_1V_{0.28}Te_{0.22}Nb_{0.07}O_n$ (Fig. 6, right). Vanadium, tellurium and molybdenum that were not a part of water soluble compounds in D_{110} and R_{190} samples dissolved in HCl. The whole of Nb in D_{110} and Nb remainder in R_{190} dissolved in HF.

So, solid precursors D_{110} and R_{190} differed by the composition of water-soluble material and a total amount of unbound elements. More specifically, D_{110} contained MoVTe compound and completely unbound Nb, on the other hand, in R_{190} approximately 50% of total Nb content was bound in a water-soluble 4-component MoVTeNb compound.

3.3.3. FT-IR spectroscopy

The infrared spectra of the solid catalyst precursors are shown in Fig. 7. The following bands could be resolved for D_{110} precursor: (i) bands at 1405vs, 928s (*925s*), 883vs (*886vs*), 673 (*678*), 620s (*615s*), 538 (*556*), 480 (*497*) and 460 (*458*) cm^{-1}, which were similar to those observed on 6-heteropolytellurate compounds with Anderson structure (shown in parenthesis) [21]; (ii) bands at 1720, 1690, 1280 and 800 cm^{-1} that could be attributed to stretching vibrations modes of C=O, a stretching combination of ν(C–O) and ν(C–C) associated with the oxalate anion (Fig. 7a). A shift of the bands related to the Mo–O bond in the Anderson-type compounds (bands at 935 and 902 cm^{-1}) for R_{190} (Fig. 7b) can tentatively be explained by a partial substitution of molybdenum by vanadium and/or niobium species in the Anderson-type anion.

3.3.4. Raman spectroscopy

Fig. 8a shows the Raman spectra of MoTe and MoVTe mixed solutions and MoVTeNb gel-like slurry in the region of M=O stretching modes. Solutions were prepared according to scheme

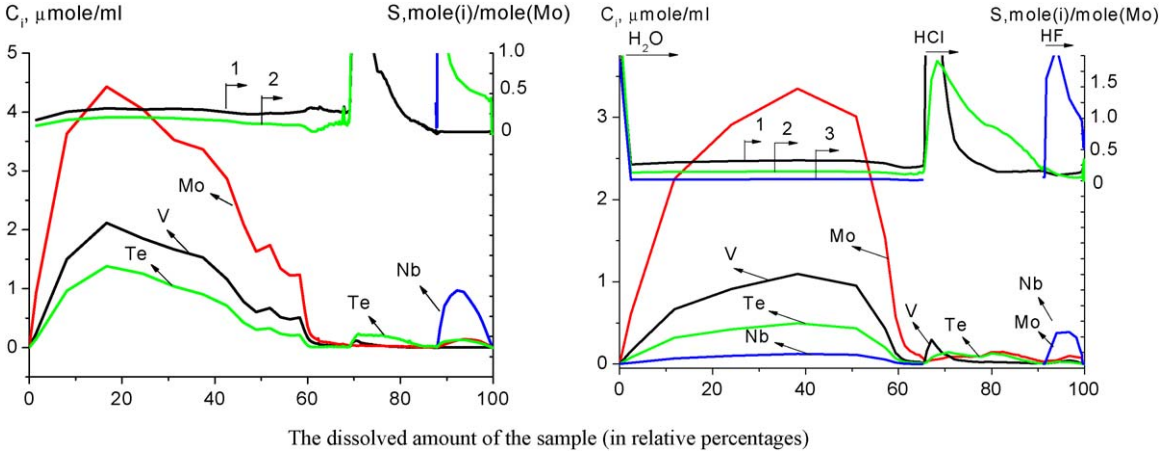

Fig. 6. The concentrations of Mo, V, Te, Nb (C_i, μmole/ml) and the corresponding stoichiograms (S, mole (i)/mole Mo) vs the dissolved amount of the sample (in relative percentages). (i) Mo, V, Te, Nb; the stoichiograms: (1) V/Mo, (2) Te/Mo, (3) Nb/Mo; (left) D_{110}, (right) R_{190}.

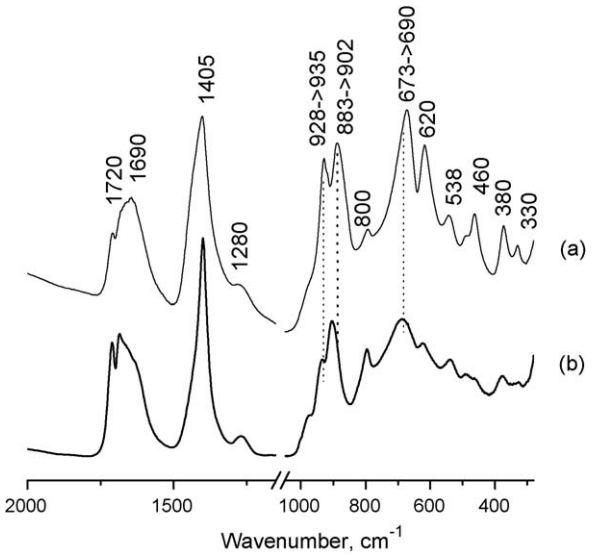

Fig. 7. FT-IR spectra of the samples in CsI matrix: (a) D_{110} and (b) R_{190}.

presented in Fig. 1. Raman bands of the MoTe mixed solution were observed at 938 and 897 cm^{-1}, which were similar to those observed in Raman spectrum of Anderson-type heteropolyanion $[TeMo_6O_{24}]^{6-}$ [21]. A new band appeared at 997 cm^{-1} after addition of ammonium metavanadate, which could be assigned to terminal V=O bonds of protonated decavanadate species $[H_xV_{10}O_{28}]^{(6-x)-}$ [12]. A similar Raman spectrum of the ternary MoVTe solution was observed in Ref. [12], in spite of a different sequence of solutions mixing (AHM + AMV + H_6TeO_6). When Nb oxalate solution was added to MoVTe solution, a gel-like slurry formed. A shift of the bands at 940, 899 and 997 cm^{-1} towards higher frequencies (945, 906 and 1006 cm^{-1}) was observed in the Raman spectrum of MoVTeNb gel. Beato et al. [12] have proposed that the shift of the stretching mode of the terminal M=O bonds was due to the formation of an Anderson-type heteropolyanion with molybdenum partially replaced by V and/or Nb.

Fig. 8b shows the Raman spectra of the solid precursors synthesized by heat evaporation (D_{110}) and spray drying (R_{190}). In the 950–850 cm^{-1} frequency range the Raman spectrum of the D_{110} solid precursors was similar to the Raman spectrum of the ternary MoVTe solution, and the Raman spectrum of the R_{190} solid precursors was identical to the Raman spectrum of the MoVTeNb gel. The bands in the high frequency region observed in MoVTe solution (997 cm^{-1}) and MoVTeNb gel (1006 cm^{-1}) disappeared in Raman spectra of solid D_{110} and R_{190} samples.

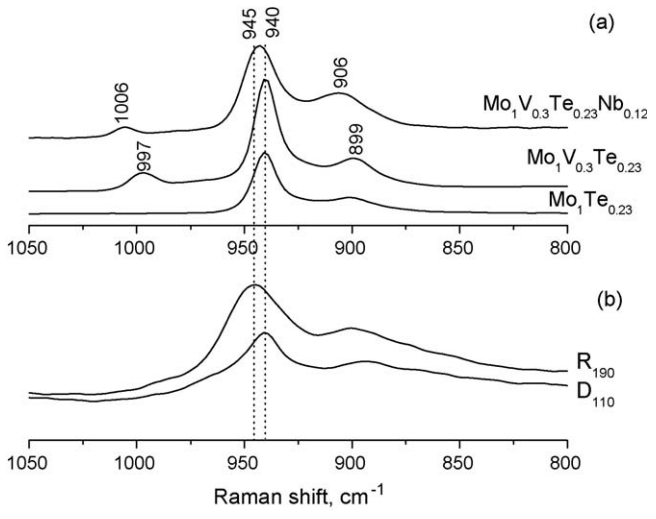

Fig. 8. Raman spectra of MoTe, MoVTe and MoVTeNb mixed solutions (a), and D_{110} and R_{190} samples (b).

4. Discussion

Overall, we have determined that the method of the slurry drying has a strong effect on the phase composition of final MoVTeNb mixed oxide catalyst and results in catalysts with highly distinct activities. The different mechanisms of phase composition formation in the samples synthesized by heat evaporation or using spray drying arise from the different chemical nature of corresponding solid precursors.

According to the FT-IR and Raman data, compounds with Anderson-type heteropolyanion structure were present in solid precursors, synthesized both by heat evaporation (D_{110}) and by spray drying (R_{190}). However, the difference in Raman and infrared spectra of D_{110} and R_{190} solid precursors (a shift of the bands of the Mo=O bond towards higher frequencies for R_{190} sample) may be caused by the formation of heteropolyanions with various chemical composition. According to the results of the differential dissolution method (DD), crystalline precursor D_{110} contained MoVTe compound and completely unbound Nb, on the other hand, the amorphous precursor R_{190} had approximately 50% of total Nb content bound in a 4-component MoVTeNb compound. In addition to DD results, we have observed that Raman spectrum of D_{110} solid precursor was similar to the spectrum of ternary MoVTe solution, and Raman spectrum of R_{190} solid precursor was identical to the spectrum of the MoVTeNb gel. Our results led us to the conclusion that R_{190} precursor, synthesized by spray drying of slurry, preserves the same properties of the starting gel. During a rapid spray drying, the entire sample is subjected to very fast concentration, which prevents selective crystallization and results in a catalyst with a more uniform composition. The uniform distribution of metal ions in the synthesis slurry remains similarly uniform in the spray-dried solid precursor and has the same stoichiometry and composition as the starting gel.

During heat evaporation we observed a change of slurry pH from 2.9 to 3.8. Oliver et al. have demonstrated that the pH of the slurry strongly affects both the crystallinity and the chemical nature of molybdotellurates [9]. Crystalline $(NH_4)_6TeMo_6O_{24}{\cdot}nH_2O$, an Anderson-type heteropolyanion, was formed in the samples prepared at pH > 3.5. In addition, it is known that pH of a solution has an effect on the niobium ion state. Niobium oxalate species hydrolyze to hydrated Nb_2O_5 and precipitate at pH > 3 [17].

The method of drying of the aqueous suspension has a pronounced effect on the phase formation of the MoVTeNb catalyst under calcination at 600 °C. Two major phases including M1 orthorhombic and M2 hexagonal phases were detected in catalyst R_{600} prepared by spray drying (Fig. 4b). M2 hexagonal, $TeMo_5O_{16}$ and $Mo_{5-x}(V/Nb)_xO_{14}$ phases were present in D_{600} sample prepared by heat evaporation (Fig. 4a).

The chemical composition and content of the phases according DD are shown in Table 2. In the D_{600} sample, more than 80% of Nb was incorporated into M2 phase and remaining Nb was incorporated into $Mo_{5-x}(V/Nb)_xO_{14}$ phase. In the R_{600} sample, practically all Nb was incorporated into M1 phase. In R_{600} sample, M2 phase was free of Nb (Table 2).

The differences in the catalytic properties of D_{600} and R_{600} samples could be attributed to different phase composition. In catalytically active and selective sample R_{600}, two crystalline phases M1 and M2 were present. According to DD, the ratio of the aforementioned phases was about 80/15. The activity of the sample D_{600} prepared by heat evaporation was low. This sample

Table 2
Phase and chemical composition, and catalytic characterization of the samples D_{600} and R_{600}.

Sample	Phase[a] composition	The component ratio[b]			Relative[b] content (%)	Catalytic characterization[c]		
		V/Mo	Te/Mo	Nb/Mo		*X* (%)[d]	*S* (%)[e]	*Y* (%)[f]
D_{600}	M2	0.38	0.27	0.27	40	17.9	57.2	10.2
	$TeMo_5O_{16}$		0.22		30			
	$Mo_{5-x}(V/Nb)_xO_{14}$	0.14		0.08	27			
	V_2O_5	3						
R_{600}	M1	0.28	0.10	0.14	80	79.6	64.2	51.1
	M2	0.30	0.35	–	15			
	$Mo_{5-x}(V/Nb)_xO_{14}$	0.11		0.07	3			

[a] According to XRD.
[b] According to DD.
[c] Reaction conditions: 1.3 g of catalyst; feed composition: 5.0% C_3H_8, 6% NH_3, balance air; total flow 33.3 ml min^{-1}; reaction temperature: 420 °C.
[d] Propane conversion.
[e] Selectivity to C_3H_3N.
[f] Yield of C_3H_3N.

did not contain the active M1 phase and consisted of some phases that were inactive in propane activation.

5. Conclusion

The method of drying, heat evaporation or spray drying, of the aqueous suspension of starting chemicals has a pronounced effect on the phase composition of the final MoVTeNb catalyst, which ultimately influences the catalytic properties in propane ammoxidation reaction.

The sample synthesized by spray drying is active and selective; it contains two main crystalline phases, orthorhombic M1 and hexagonal M2. The activity of the sample prepared by heat evaporation is low. This sample does not contain the active M1 phase and consists of hexagonal M2, $TeMo_5O_{16}$, and $Mo_{5-x}(V/Nb)_xO_{14}$ phases.

The different mechanisms of phase composition formation in the samples synthesized by heat evaporation or spray drying arise from the different chemical nature of corresponding solid precursors.

References

[1] T. Ushikubo, K. Oshima, A. Kayou, T. Umezawa, K. Kiyono, I. Sawaki, Mitsubishi Chem. Corp., EP Patent EP 529,853 (1993).
[2] T. Ushikubo, Y. Koyasu, S. Wajiki, Mitsubishi Chem. Corp., EP Patent 608,838 (1994).
[3] T. Ushikubo, K. Oshima, A. Kayou, M. Vaarkamp, M. Hatano, J. Catal. 169 (1997) 394.
[4] M. Aouine, J.L. Dubois, J.M.M. Millet, Chem. Commun. 194 (2001) 1180.
[5] H. Tsuji, Y. Koyasu, J. Am. Chem. Soc. 124 (2002) 5608.
[6] D. Vitry, Y. Morikawa, J.L. Dubois, W. Ueda, Top. Catal. 23 (2003) 47.
[7] P. Botella, E. Garcia-Gonzalez, J.M. López Nieto, J.M. Gonzalez-Calbet, Solid State Sci. 7 (2005) 507.
[8] M.M. Lin, Appl. Catal. A: Gen. 250 (2003) 305.
[9] J.M. Oliver, J.M. Lopez Nieto, P. Botella, A. Mifsud, Appl. Catal. A: Gen. 257 (2004) 67.
[10] F. Ivars, P. Botella, A. Dejoz, J.M. López Nieto, P. Concepcion, M.I. Vazques, Top. Catal. 38 (2006) 59.
[11] G.Ya. Popova, T.V. Andrushkevich, G.I. Aleshina, L.M. Plyasova, M.I. Khramov, Appl. Catal. A: Gen. 328 (2007) 195.
[12] P. Beato, A. Blume, F. Girgsdise, R.E. Jentoft, R. Schlögl, O. Timpe, A. Trunschke, G. Weinberg, Q. Basher, F.A. Hamid, S.B.A. Hamid, E. Omar, L. Mohd Salim, Appl. Catal. A: Gen. 307 (2006) 137.
[13] V.V. Malakhov, A.A. Vlasov, L.S. Dovlitova, Zh. Anal. Khim. 59 (2004) 1126–1137; V.V. Malakhov, A.A. Vlasov, L.S. Dovlitova, J. Anal. Chem. (Engl. Transl.) 59 (2004) 1014.
[14] V.V. Malakhov, I.G. Vasilyeva, Russ. Chem. Rev. 77 (2008) 350.
[15] (a) T. Ushikubo, K. Oshima, A. Kayo, M. Hatano, Stud. Surf. Sci. Catal. 112 (1997) 473;
(b) P. Botella, J.M. Lopez Nieto, B. Solsona, Catal. Lett. 78 (2002) 383.
[16] ICDD [31-874].
[17] AC ICDD [57-1100].
[18] (a) P. DeSanto Jr., D.J. Buttrey, R.K. Grasselli, C.G. Lugmair, A.F. Volpe, B.N. Toby, T. Vogt, Top. Catal. 23 (2003) 23;
(b) H. Mirayama, D. Vitry, W. Ueda, G. Fuchs, M. Anne, J.L. Dubois, Appl. Catal. A: Gen. 318 (2007) 137.
[19] H.T. Evans Jr., J. Am. Chem. Soc. (1968) 3275.
[20] Y.H. Sun, J. Liu, E. Wang, Inorg. Chim. Acta 117 (1986) 23.
[21] (a) I.L. Botto, C.I. Cabello, H.J. Tomas, Mater. Chem. Phys. 47 (1997) 37;
(b) R. Ratheesh, G. Suresh, V.U. Nayar, J. Solid State Chem. 18 (1995) 341.